J|A|C|S
COMMUNICATIONS

Published on Web 02/16/2007

Interparticle Influence on Size/Size Distribution Evolution of Nanocrystals

Jason Thessing,[†] Jianghong Qian,[†] Haiyan Chen,[‡] Narayan Pradhan,[†] and Xiaogang Peng*,[†]

Department of Chemistry and Biochemistry, University of Arkansas, and NN-Labs, LLC, Fayetteville, Arkansas 72701

Received November 11, 2006; E-mail: xpeng@uark.edu

The understanding of crystallization has played a decisive role in developing synthetic chemistry for high-quality nanocrystals both in solution[1−3] and on substrates.[4] Semiconductor nanocrystals have been used as the main models for studying nanocrystal formation due to their size-dependent optical properties, both photoluminescence (PL) and UV−vis.[5,6] Their PL spectra are usually a single-peak, but PL quantum yield may differ from one size to another in a sample and vary greatly by changing the chemical environment.[7,8] UV−vis is normally not sensitive to the environment, but it is a superposition of different peaks even for a monodisperse sample.[9] As a result, such studies have been qualitative or semiquantitative, although in situ[10] and microfluidic[11] methods have been developed for accurately recording UV−vis and PL spectra. This work intends to solve this challenge by quantitatively deconvoluting UV−vis spectra of semiconductor nanocrystals with a series of standard spectra. Initial results obtained using this new technique imply that interparticle interaction needs to be considered in size/size distribution evolution of nanocrystals although this parameter has been largely ignored in the past.

CdS and CdSe nanocrystals were synthesized using standard methods.[7,12] For computer deconvolution, 45 standard UV−vis spectra of CdS nanocrystals were collected (Figures 1a and S1), with one spectrum for every 2−3 nm interval. For most experiments (Supporting Information (SI)), CdS nanocrystals were treated with tolusulfonic acid in octanol at ambient conditions in a sealed cuvette, and the UV−vis spectra were recorded in situ using an Ocean Optics fiber-optic spectrophotometer.

Each spectrum was deconvoluted by fitting it with the standard spectra using Monte Carlo simulation (SI). The simulation protocol was examined by the excellent fitting (Figure 1b, c, d) of the spectra of a standard sample, and a mixture of either two or three standard samples. The monomer concentrations and size distribution obtained from the deconvolution were confirmed for a few samples by atomic absorption and TEM (see below), respectively.

The Gibbs−Thompson equation is shown in eq 1.[13]

$$S_d = S_\infty \exp(4\sigma V_m/dRT) \quad (1)$$

σ and V_m are the specific surface energy and molar volume of a crystal, respectively. S_∞ is the solubility of the bulk crystal, and S_d is that for a crystal with its diameter as d. R is the gas constant, and T is absolute temperature. For a given sized nanocrystal, it dissolves (grows) if the monomer concentration in solution is lower (higher) than its solubility determined by eq 1,[13,14] which is known as Ostwald ripening.[13]

When the acid was injected into the nanocrystal solution, net dissolution occurred instantaneously (Figure 2a, 0−10 s)—indicated by the blue-shift and intensity decrease of the absorption spectrum—because the monomer concentration in solution was initially zero. Subsequently, the average size increased, judged by the UV−vis peak position, and the particle concentration continued to decrease (>10 s). All these qualitative features matched well with a typical Ostwald-ripening process, which is confirmed by the quantitative results (Figure 2b) obtained by deconvoluting the UV−vis spectra. The transition point from net dissolution to net growth of average size is indicated by a red line in Figure 2b, and the related monomer concentration, $[M]^t$ should be the solubility of an average-sized crystal in the solution according to eq 1.

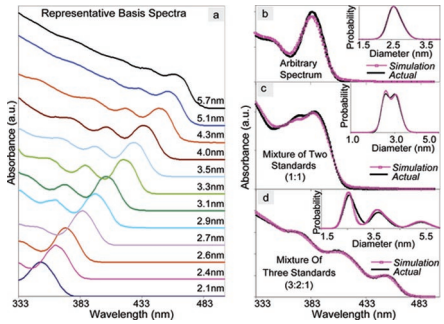

Figure 1. (a) Representative standard spectra of CdS nanocrystals. (b−d) Comparison of simulated spectra and size distribution with the experimental results for single size and mixtures.

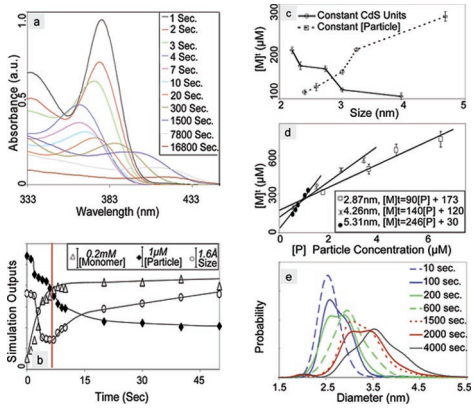

Figure 2. (a) Temporal evolution of UV−vis spectra and (b) corresponding parameters obtained by deconvolution of a CdS nanocrystal sample in the acid solution. (c, d) $[M]^t$ at different conditions. (e) Size distribution evolution in dissolution/ripening.

However, additional experimental results with differently sized nanocrystals reveal that $[M]^t$ is unlikely the solubility of the nanocrystals. In Figure 2c, two opposite trends can be identified, a decrease of $[M]^t$ for a low particle concentration (constant CdS units for all sizes) and an increase of $[M]^t$ for a high particle concentration (constant initial [particle] for all sizes). To clarify this conflict, $[M]^t$ with different particle concentrations was examined (Figure 2d). A linear increase of $[M]^t$ over the increase of [particle] occurred for all sizes.

To confirm the role of particle concentration in ripening, one CdS nanocrystal sample (405 nm UV−vis peak) was subjected to ripening with/without another size (368 nm UV−vis peak). The

[†] University of Arkansas.
[‡] NN-Labs, LLC.

10.1021/ja068072z CCC: $37.00 © 2007 American Chemical Society

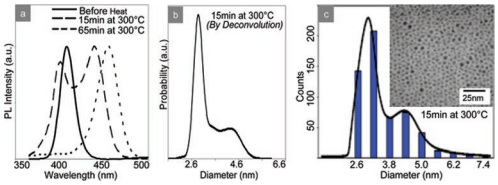

Figure 3. Ostwald ripening of CdS nanocrystals at 573 K in oleic acid−octadecene solution. (a) PL spectra at three reaction times. (b) Size distribution at 15 min by the deconvolution of the corresponding UV−vis spectrum. (c) Size distribution at 15 min determined by TEM.

results (Figure S2, top) indicate that the existence of the small nanocrystals almost prevented the dissolution of the large ones. This implies that the large particles "felt" the existence of the small ones. The related results also confirm that focusing of size distribution[14] may occur more substantially (Figure S2, bottom) in ripening than that predicted by the theories.[20,21]

The temporal evolution of size distribution of the nanocrystals in ripening (Figure 2e) showed a bimodal distribution as transient states, instead of a constant log-normal distribution predicted by Lifshitz−Slyozov−Wagner (LSW) theory.[15,16] Such bimodal distribution seems to be common as shown by further experiments using different nanocrystals and/or with different temperature/solvent systems (Figure 3 and Figure 3S). In some cases, the nanocrystals emitted well, which offered an opportunity for comparing size distribution profiles implied by the PL spectrum and determined by deconvolution of the UV−vis. Evidently, the size distribution determined by computer deconvolution of UV−vis (Figure 3b) was substantially more accurate than that implied by the PL spectrum (Figure 3a) using TEM results as the reference (Figure 3c). This is consistent with dynamic distribution of PL brightness of nanocrystals.[7,8]

Equation 1 and LSW theory[15,16] cannot directly explain the results in Figure 3. However, study of Ostwald ripening on solid substrates for two-dimensional (2D) nanosized islands revealed that the behavior of a given island was determined by the size and distance of its nearest neighbor islands,[17,18] which was quantitatively explained by considering the inter-island diffusion of monomers based on Gibbs−Thompson equation. In our case, the interparticle distance was estimated as several tens of nanometers, which should allow significant diffusion sphere overlapping. This implies that, for a diffusion controlled process (commonly assumed for most studies of colloidal nanocrystals) the interparticle diffusion (the second term in eq 2), in addition to the well-known solution−particle diffusion (the first term in eq 2),[14,19−21] might also play a key role in determining the size growth rate (d') of a nanocrystal in solution.

$$d' = 10\mathrm{D}\pi q^2(S_{\mathrm{ave}} - S_{\mathrm{d}})[\mathrm{P}] + 4D/d([\mathrm{M}] - S_{\mathrm{d}}) \qquad (2)$$

($[\mathrm{M}] - S_{\mathrm{d}}$): monomer concentration gradient between the bulk solution and a given nanocrystal, ($S_{\mathrm{ave}} - S_{\mathrm{d}}$): mean interparticle diffusion gradient (SI), D: diffusion coefficient of monomers, q: radius of the diffusion sphere, and [P]: particle concentration. This preliminary model and interpretation below only requires solubility of nanocrystals to increase with the decrease of their size. Previous theoretical reports treated the growth of nanocrystals using a form of the Gibbs−Thompson equation[20,21] more precise than that in LSW theory, but particle−particle interactions are not yet considered. At dissolution−growth transition, d' equals to zero, and $[\mathrm{M}]^{\mathrm{t}}$ can be determined by eq 3.

$$[\mathrm{M}]^{\mathrm{t}} = (5\pi q^2/2)\, d\, (S_{\mathrm{d}} - S_{\mathrm{ave}})[\mathrm{P}] + S_{\mathrm{d}} \qquad (3)$$

Equation 3 implies a linear relationship between $[\mathrm{M}]^{\mathrm{t}}$ and [P], and the slope should increase with the size (d) of the nanocrystals. These two predictions are quantitatively consistent with the data in Figure 2d. The solubility (S_{d}) of nanocrystals determined by the y-axis intercept for each line in Figure 2d increases as the particle size decreases, which is consistent with the initial assumption. Equations 2 and 3 further indicate that, as the size-dependent solubility becomes insignificant for large particles, the interparticle diffusion becomes negligible because ($S_{\mathrm{ave}} - S_{\mathrm{d}}$) approaches zero. This is probably why interparticle interaction is readily observable in nanosize range.

The second term in eq 2 is always positive (negative) for the particles bigger (smaller) than the average size. As the large particles started growing, the ones smaller than the critical size determined by eq 3 would still dissolve rapidly, much more so than that predicted by eq 1. Thus, a gap was developed between the large particles in growth and small ones in rapid dissolution. After the bimodal distribution (Figures 2e and 3a), or starting from a broad distribution (Figure S2), focusing of size distribution will follow due to the complete dissolution of the small particles.

In summary, quantitative study of crystallization in a few-nanometer-sized regime is critically important but has been extremely challenging. The technique reported here offers the possibility for experimentally solving this challenge, and the initial results are encouraging. Interparticle interaction was for the first time identified as a determining role in Ostwald ripening of colloidal nanocrystals although related phenomena were observed previously for relatively larger sized crystals in melts with high solid/volume ratio[22] and 2D islands on substrate.[17,18] The preliminary model proposed can explain the observed experimental results, i.e., the concentration-dependent transition of dissolution to ripening, bimodal size distribution, and focusing of size distribution in ripening. A more precise theory is under development, which should impact several fields in science and technology, such as chemistry, biology, geology, and materials.

Supporting Information Available: Experimental details and supporting results. This material is available free of charge via the Internet at http://pubs.acs.org.

References

(1) Murray, C. B.; Kagan, C. R.; Bawendi, M. G. *Annu. Rev. Mater. Sci.* **2000**, *30*, 545−610.
(2) Peng, X.; Thessing, J. *Struct. Bonding* **2005**, *118*, 79−119.
(3) Im, S. H.; Lee, Y. T.; Wiley, B.; Xia, Y. *Angew. Chem.* **2005**, *44*, 2154−2157.
(4) Tian, Z. R.; Voigt, J. A.; Liu, J.; McKenzie, B.; McDermott, M. J.; Rodriguez, M. A.; Konishi, H.; Xu, H. *Nat. Mater.* **2003**, *2*, 821−826.
(5) Alivisatos, A. P. *Science* **1996**, *271*, 933−937.
(6) Brus, L. E. *J. Chem. Phys.* **1983**, *79*, 5566−5571.
(7) Qu, L.; Peng, X. *J. Am. Chem. Soc.* **2002**, *124*, 2049−2055.
(8) Talapin, D. V.; Rogach, A. L.; Shevchenko, E. V.; Kornowski, A.; Haase, M.; Weller, H. *J. Am. Chem. Soc.* **2002**, *124*, 5782−5790.
(9) Yu, W. W.; Qu, L.; Guo, W.; Peng, X. *Chem. Mater.* **2003**, *15*, 2854−2860.
(10) Qu, L.; Yu, W. W.; Peng, X. *Nano Lett.* **2004**, *4*, 465−469.
(11) Chan, E. M.; Mathies, R. A.; Alivisatos, A. P. *Nano Lett.* **2003**, *3*, 199−201.
(12) Yu, W. W.; Peng, X. *Angew. Chem.* **2002**, *41*, 2368−2371.
(13) Mullin, J. W. *Crystallization*, 3rd ed.; Butterworth-Heinemann: Boston, 1997.
(14) Peng, X.; Wickham, J.; Alivisatos, A. P. *J. Am. Chem. Soc.* **1998**, *120*, 5343−5344.
(15) Lifshitz, I. M.; Slyozov, V. V. *J. Phys. Chem. Solids* **1961**, *19*, 35−50.
(16) Wagner, C.; Z. Elektrochemie *Angew. Phys. Chem.* **1961**, *65*, 581−91.
(17) Rosenfeld, G.; Morgenstern, K.; Esser, M.; Comsa, G. *Appl. Phys. A* **1999**, *69*, 489−496.
(18) Morgenstern, K.; Rosenfeld, G.; Comsa, G. *Surf. Sci.* **1999**, *441*, 289−300.
(19) Peng, Z. A.; Peng, X. *J. Am. Chem. Soc.* **2001**, *123*, 1389−1395.
(20) Talapin, D. V.; Rogach, A. L.; Haase, M.; Weller, H. *J. Phys. Chem. B* **2001**, *105*, 12278−12285.
(21) Mantzaris, N. V. *Chem. Eng. Sci.* **2005**, *60*, 4749−4770.
(22) Alkemper, J.; Snyder, V. A.; Akaiwa, N.; Voorhees, P. W. *Phys. Rev. Lett.* **1999**, *82*, 2725−2728.

JA068072Z